Elastic stability of Ga_2O_3: Addressing the β to α phase transition from first principles

Konstantin Lion, Pasquale Pavone, and Claudia Draxl*
Institut für Physik and IRIS Adlershof, Humboldt-Universität zu Berlin, 12489 Berlin, Germany

(Received 2 September 2021; accepted 2 December 2021; published 3 January 2022)

The elastic and structural properties of β-Ga_2O_3 and α-Ga_2O_3 are investigated from first principles. The full elastic tensors and elastic moduli of both phases at 0 K are computed in the framework of semilocal density-functional theory. We determine mechanical instabilities of β-Ga_2O_3 by evaluating the full stiffness tensor under load for a range of hydrostatic pressure values. While a phase transition from the β to α phase is found to be energetically favored at 2.6 GPa, we show that the β phase is mechanically unstable only for much higher pressures (>30 GPa), which agrees well with experimental results. Our employed approach is based on the Born stability criterion, is independent of crystal symmetry, and thus can be readily applied to different materials.

DOI: 10.1103/PhysRevMaterials.6.013601

I. INTRODUCTION

The wide-gap transparent conducting oxide gallium oxide (Ga_2O_3) has gained a lot of interest in recent years as a potential candidate for a number of applications. Its tunable electrical and optical properties make it a promising material for gas sensors [1–5], field-effect transistors [6], and photodetectors [7–10]. The material exhibits polymorphism; that is, depending on the experimental conditions, it can adopt one out of at least five different known structures (α, β, γ, δ, and ϵ) [11]. The thermodynamically stable phase at ambient conditions is β-Ga_2O_3. It crystallizes in a base-centered monoclinic structure (space group $C2/m$) and consists of both tetrahedrally and octahedrally coordinated gallium atoms. The metastable high-density α phase exhibits a rhombohedral corundum structure (space group $R\bar{3}c$) and is made up of solely octahedrally coordinated gallium. The unit cells of α- and β-Ga_2O_3 are illustrated in Fig. 1. Remeika and Marezio first reported a phase transition of the β phase to the α phase at 4.4 GPa and 1000 K [12]. The transformation was found to be irreversible after quenching the sample to room temperature. Since then, the phase transition has been the subject of several studies at both high and room temperatures. Studying nanoparticles of β-Ga_2O_3 embedded in an amorphous silica-based host matrix by synchrotron-radiation-based x-ray diffraction [13], Lipinska-Kalita and coworkers reported a phase transition that sets in at about 6 GPa and is not completed at 15 GPa. It is, however, not clear whether the phase transition is affected by the host matrix or intrinsic to the nanoparticles [13]. In a follow-up study conducted on bulk β-Ga_2O_3 at pressures up to 70 GPa, they reported an onset of 7.9 GPa (3 GPa) and the completion of the transition at 40 GPa (30 GPa) with (without) nitrogen as a pressure-transmitting medium [14]. Wang and coworkers subsequently subjected freestanding β-Ga_2O_3 nanocrystals to pressures up to 64.9 GPa at room temperature and reported a transition onset between 13.6 and 16.4 GPa and a completed transition at 39.2 GPa [15]. A phase transition was also observed in β-Ga_2O_3 microparticles, taking place between 20 and 39 GPa, where only a highly disordered structure comparable to α-Ga_2O_3 remained [16]. Also in recently reported shock-recovery experiments, a phase transition occurred (between 11 and 16 GPa) [17]. Similar transition pressures have been published in computational studies. The reported values range from 2 to 17 GPa [18–21].

From the review above, it is apparent that while there is an extensive discussion in the literature about the phase transition between the two polymorphs, the pressure at which the transition takes place is far from being settled. In particular, the interplay between the transition pressure p_t, which is obtained by thermodynamical considerations, and the critical pressure p_c, which is ruled by a mechanical instability, has not been thoroughly discussed. This is the aim of our work, in which we illustrate that only considering both allows for understanding the diversity of experimental results. We investigate the β to α phase transition by calculating the elastic properties of both α- and β-Ga_2O_3 and examining, in particular, their variation under hydrostatic pressure. The critical pressure is obtained by applying the generalized Born stability criterion to the elastic constants under load.

II. THEORETICAL BACKGROUND

Application of strain leads to deformation of the crystal due to the resulting stress. In the linear elastic regime, strain and stress can be represented by symmetric second-rank tensors and are related by Hooke's law [22–24],

$$\sigma_{ij} = C_{ijkl}\,\epsilon_{kl}, \tag{1}$$

where C_{ijkl} represents the stiffness tensor, ϵ_{kl} is the physical strain tensor, and σ_{ij} is the stress tensor. For conciseness, we employ Einstein's notation for summations throughout this work. When dealing with symmetric tensors, it is convenient to use the Voigt notation, where a pair of Cartesian indices ij

*claudia.draxl@physik.hu-berlin.de

can be written as a single index γ, according to

ij	11	22	33	23	13	12
γ	1	2	3	4	5	6

In the following, tensors expressed in the Voigt notation are represented by six-dimensional vectors using a bold font. In order to calculate the stiffness tensor, one can expand the total crystal energy per unit cell $E(\boldsymbol{\epsilon})$ in terms of the strain [25],

$$\frac{E(\boldsymbol{\epsilon})}{V_0} = \frac{E_0}{V_0} + \underbrace{\boldsymbol{\sigma}_0 \cdot \boldsymbol{\epsilon}}_{=0} + \frac{1}{2!}\,\boldsymbol{\epsilon}^{\mathsf{T}} \cdot \boldsymbol{C} \cdot \boldsymbol{\epsilon} + \cdots, \tag{2}$$

where E_0 and V_0 refer to the equilibrium energy and volume per unit cell and $\boldsymbol{\sigma}_0$ refers to the equilibrium stress tensor. The stiffness tensor is defined as

$$C_{\gamma\lambda} = \frac{1}{V_0}\,\frac{\partial^2 E(\boldsymbol{\epsilon})}{\partial\,\epsilon_\gamma\,\partial\,\epsilon_\lambda}\bigg|_{\boldsymbol{\epsilon}=0}. \tag{3}$$

This definition is only valid for the description of an initially unstressed crystal. For a crystal under arbitrary constant stress, it is necessary to introduce a stiffness tensor under load B_{ijkl}. As hydrostatic pressure does not reduce the crystal symmetry, it has the same symmetry as the stiffness tensor $\boldsymbol{C}$ and can be represented in Voigt notation, henceforth denoted as $\boldsymbol{B}$. The appropriate thermodynamical potential to describe the stressed system is the enthalpy $H = E + p_0 V$, where p_0 represents the initial constant pressure. The stiffness tensor under external hydrostatic pressure can then be calculated as

$$B_{\gamma\lambda} = \frac{1}{\widetilde{V}_0}\,\frac{\partial^2 H(\boldsymbol{\epsilon})}{\partial\,\epsilon_\gamma\,\partial\,\epsilon_\lambda}\bigg|_{\boldsymbol{\epsilon}=0}, \tag{4}$$

where $\widetilde{V}_0$ is the volume per unit cell for the initially stressed structure. To derive the relation between $C_{\gamma\lambda}$ and $B_{\gamma\lambda}$, we have to transform back to Cartesian indices and start with arbitrary constant external stress σ_{ij}. B_{ijkl} can then be expressed as [23,26,27]

$$B_{ijkl} = \widetilde{C}_{ijkl} + \tfrac{1}{2}(\delta_{ik}\,\sigma_{jl} + \delta_{jk}\,\sigma_{il} + \delta_{il}\,\sigma_{jk} + \delta_{jl}\,\sigma_{ik} - 2\,\delta_{kl}\,\sigma_{ij}). \tag{5}$$

Note that now one has to evaluate the stiffness tensor $\widetilde{C}_{ijkl}$ for the initially stressed crystal configuration at volume $\widetilde{V}_0$. In this work, we consider the β phase under external hydrostatic pressure, $\sigma_{ij} = -P\,\delta_{ij}$ ($P > 0$ for tension). Then, the stiffness tensor under load can be written as

$$B_{ijkl} = \widetilde{C}_{ijkl} - P(\delta_{ik}\,\delta_{jl} + \delta_{jk}\,\delta_{il} - \delta_{kl}\,\delta_{ij}). \tag{6}$$

Both tensors have the same symmetry, and we can thus go back to Voigt notation. It follows that

$$B_{\gamma\lambda} = \widetilde{C}_{\gamma\lambda} + \begin{pmatrix} -P & P & P & 0 & 0 & 0 \\ P & -P & P & 0 & 0 & 0 \\ P & P & -P & 0 & 0 & 0 \\ 0 & 0 & 0 & -P & 0 & 0 \\ 0 & 0 & 0 & 0 & -P & 0 \\ 0 & 0 & 0 & 0 & 0 & -P \end{pmatrix}. \tag{7}$$

The Born stability criterion [28] enables us to determine the elastic stability of an unstressed crystal: A crystal with arbitrary symmetry is stable if the stiffness tensor $\boldsymbol{C}$ is positive definite [28,29]. This condition is equivalent to $\boldsymbol{C}$ being a symmetric tensor having only positive eigenvalues that can be calculated with standard algebraic techniques. While the Born stability criterion is formulated for an unstressed crystal, it can also be generalized to the case of constant external hydrostatic load; in this case, the stiffness tensor under load $\boldsymbol{B}$ has to be positive definite [29].

III. COMPUTATIONAL DETAILS

All calculations are performed in the framework of density-functional theory using the all-electron full-potential code `exciting` [30], which applies the linearized augmented plane wave plus local orbital method. Exchange-correlation effects are treated within the generalized gradient approximation as parametrized by Perdew-Burke-Ernzerhof for solids and surfaces (PBEsol) [31], which shows high accuracy in determining elastic properties for solids [32]. Total energies are calculated using an $8 \times 8 \times 8$ ($6 \times 6 \times 6$) **k** grid and a plane wave cutoff $R_{\mathrm{MT}}^{\mathrm{min}}\,G_{\mathrm{max}} = 9.0$ for α-Ga_2O_3 (β-Ga_2O_3). We employ muffin-tin radii of $R_{\mathrm{MT}}^{\mathrm{Ga}} = 1.65a_0$ ($1.75a_0$) and $R_{\mathrm{MT}}^{\mathrm{O}} = 1.45a_0$ for gallium and oxygen, respectively, in α-Ga_2O_3 (β-Ga_2O_3), where a_0 is the Bohr radius. The internal atomic positions are relaxed until the atomic forces are smaller than 0.2 mHa a_0^{-1}. These parameters ensure a numerical precision of $10^{-2}a_0^3$ for the equilibrium volume V_0, 10^{-2} GPa for the bulk modulus B_0, and 10^{-3} for its pressure derivative B_0'.

In order to calculate the full stiffness tensor at zero pressure, a total of 13 (6) different deformation types are applied to β-Ga_2O_3 (α-Ga_2O_3). The reader is referred to Ref. [25] for a full list of the employed deformation types. For each of them, several equally spaced strain points around the origin are created for physical strain up to 4.5%. For every deformed structure, the internal atomic positions are relaxed until the atomic forces are smaller than 0.2 mHa a_0^{-1}. The preparation of the deformed structures and evaluation of second-order derivatives shown in Eqs. (3) and (4) are performed using the `ElaStic` tool [25]. We create eight deformed β-Ga_2O_3 structures to analyze the variation of the elastic constants under strain. The corresponding pressure values are extracted from the energy vs volume fit and range from -10 to 35 GPa.

IV. RESULTS AND DISCUSSION

A. Structural properties

The lattice parameters, bulk moduli B_0, and their pressure derivatives B_0' are obtained as fitting parameters from the Birch-Murnaghan equation of state (EOS). The results for the α and β phases are given in Table I. All parameters, obtained at zero temperature and pressure, show excellent agreement with previously published theoretical and experimental work. The bulk modulus of the α phase is larger than that of the β phase by about 50 GPa. Considering that α-Ga_2O_3 is the more compressed phase and the bulk modulus is a measure of resistance against uniform compression, such a result is expected. Compared to experiment, it is underestimated by about 10%–20%, which is within the typical accuracy of a semilocal density-functional theory calculation of elastic properties [34]. Note that B_0 here is obtained from a fit and not

TABLE I. Calculated lattice parameters, a, b, and c (in Å); monoclinic angle β (in degrees); bulk moduli B_0 (in GPa); and their pressure derivatives B_0' of α-Ga_2O_3 and β-Ga_2O_3 at zero pressure.

α-Ga_2O_3	a	c	B_0	B_0'		
Present work	5.01	13.47	218	4.5		
Theory [19] (LDA)	4.95	13.32	244	3.8		
Theory [20] (AM05)	5.00	13.45	215	4.5		
Experiment [14]	4.98	13.43	252	4		
β-Ga_2O_3	a	b	c	β	B_0	B_0'
Present work	12.30	3.05	5.82	103.7	169	3.9
Theory [33] (LDA)	12.21	3.03	5.75	103.6	219	3.2
Theory [20] (AM05)	12.30	3.05	5.81	103.7	165	3.8
Experiment [14]	12.23	3.04	5.80	103.8	184	4

explicitly calculated as a linear combination of second-order elastic constants (see Sec. IV C).

B. Phase transition

Using the energy vs volume relation at high pressures, we can further analyze the phase transition from the β to the α phase. The Gibbs free energy, $G = U + pV - TS$, dictates the structural stability at a given temperature and pressure. The complete calculation of this quantity would require the full phonon spectrum. In this work, we focus on the enthalpy $H = E + pV$, i.e., the low-temperature case, where the internal energy, $U \approx E$, is determined by the Birch-Murnaghan EOS. Such an approach is justified for the pressure-induced properties of hard materials [35]. For a given pressure, the crystal phase with the lowest enthalpy is the most stable one, while a crossing point between two phases indicates a first-order phase transition. This transition pressure is purely obtained by thermodynamical considerations and will henceforth be denoted as p_t.

The calculated Birch-Murnaghan EOSs for both phases are given in Fig. 2. We obtain a transition pressure of $p_t = 2.6$ GPa. This value can be compared with the experimental transition onset, owing to the fact that a new phase is thermodynamically favored once this pressure is reached. We therefore consider p_t to be the lower bound for a phase transition setting in. As illustrated in the Introduction, the discrepancy between published transition pressures is quite high as the experimental conditions play a vital role in determining the transition onset, where temperature, pressure medium, sample size, and type can have a dramatic impact. Consequently, reported experimental values range from 3 to 20 GPa [13,14,16,17,36]. However, also theoretical values range from 2 to 17 GPa [18–21]. Here, differences can be assigned to the usage of different exchange-correlation functionals as well as as the treatment of the Ga 3d states (as core or valence states) in pseudopotential approaches.

C. Elastic stability at different pressures

1. Ambient pressure

Depending on the crystal symmetry, the stiffness tensor can have up to 21 independent components. In the case of the monoclinic β phase (rhombohedral α phase), this number reduces to 13 (6). The calculated second-order elastic constants at zero pressure for both phases are summarized in Tables II and III, showing excellent agreement with other theoretical results. To compare our results to those of Ref. [20], we employ

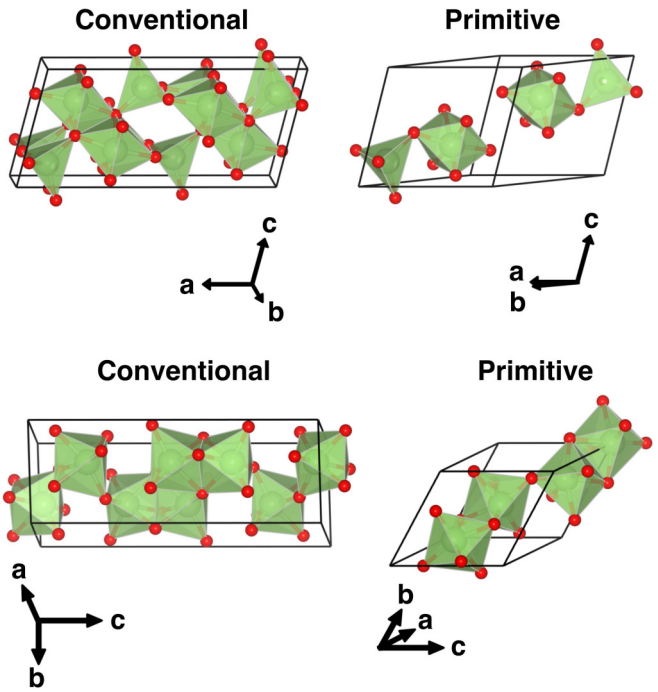

FIG. 1. Top: Conventional (left) and primitive (right) unit cell of β-Ga_2O_3. Bottom: Same for α-Ga_2O_3. Gallium atoms are in green; oxygen atoms are in red.

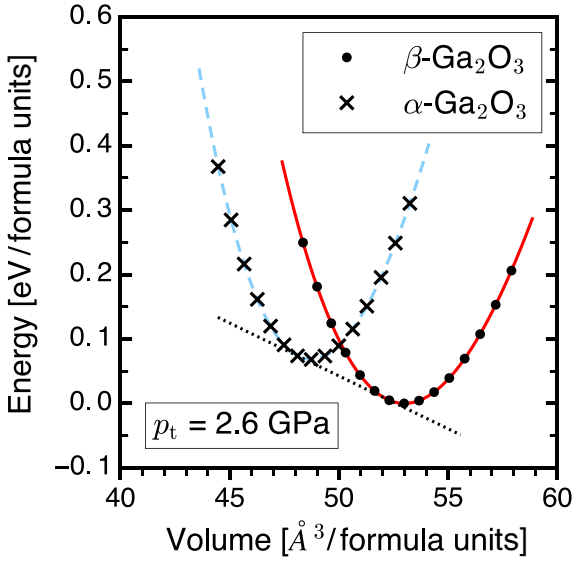

FIG. 2. Equations of state for the α and β phases of Ga_2O_3. Energies are relative to values of β-Ga_2O_3. The dots and crosses are the computed data points for β-Ga_2O_3 and α-Ga_2O_3, respectively. The solid and dashed lines represent the corresponding Birch-Murnaghan fits. The dotted line represents the common tangent of the EOS for both phases. The transition pressure p_t is determined by the common gradient.

TABLE II. Calculated second-order elastic constants at ambient pressure for the β phase of Ga_2O_3 (in GPa) compared to previously published results.

β-Ga_2O_3	C_{11}	C_{12}	C_{13}	C_{15}	C_{22}	C_{23}	C_{25}	C_{33}	C_{35}	C_{44}	C_{46}	C_{55}	C_{66}
Present work	220.5	116.4	128.3	−17.3	329.5	79.1	11.4	326.8	7.2	50.0	18.1	66.1	91.5
Theory [20]	223.1	116.5	125.3	−17.4	333.2	75.0	12.2	330.0	7.3	50.3	17.4	68.6	94.2
Experiment [37]	242.8	128.0	160.0	−1.6	343.8	70.9	0.4	347.4	1.0	47.8	5.6	88.6	104.0

the same lattice representation. For β-Ga_2O_3 it is chosen such that the y axis is parallel to b, the x axis is parallel to a, and the c axis lies in the x-z plane (see Fig. 1).

We also calculate the elastic moduli as linear combinations of second-order elastic constants and compare the bulk modulus with the one obtained from the Birch-Murnaghan EOS, B_0, shown in Table IV. The values for the bulk moduli from both methods show excellent agreement, further validating the precision of our calculations. All elastic moduli of the β phase are smaller than those of the α phase. This is expected since the latter is obtained from compressing β-Ga_2O_3 under hydrostatic strain, and a higher density leads to more resistance against strain and therefore larger elastic moduli.

The second-order elastic constants of both phases exhibit pronounced anisotropy due to crystal symmetry. The diagonal terms, C_{11}, C_{22}, and C_{33}, have the highest values, in excess of 200 GPa. As large diagonal components mean a high degree of hardness against strain in the respective directions, both phases strongly resist deformations along the main axes. This situation is reversed for the shear-strain components (indices 4 to 6). The calculated values are much smaller than the axial strain components (indices 1 to 3). They are as low as $C_{25} = 11.4$ GPa and $C_{35} = 7.2$ GPa for the β phase and $C_{14} = -16.5$ GPa for the α phase. These findings suggest that both phases are susceptible to shear strains. The elastic moduli further validate this assumption, as the shear modulus for both phases is smaller than the bulk and Young moduli, i.e., $G < B < E$.

Importantly, for both the β and α phases, all eigenvalues of the stiffness tensors are positive. Thus, according to the Born stability criterion, they are elastically stable at equilibrium at 0 K. This coincides with previously published results [11], where β-Ga_2O_3 was identified as the thermodynamically stable phase and α-Ga_2O_3 was identified as a metastable phase.

2. Variation under hydrostatic pressure

We now explore how the second-order elastic constants of the β phase react to hydrostatic pressure. For this purpose, we perform calculations on configurations that are obtained by isotropically straining the crystal by applying the transformation

$$\boldsymbol{R}(\epsilon) = (1+\epsilon)\boldsymbol{R}_{P=0},$$

where ϵ is a constant value, and calculate their stiffness tensors under load $\boldsymbol{B}$ [Eq. (4)]. The chosen values for ϵ correspond to pressure values between −10 and +35 GPa. The results are summarized in Table V. Overall, the elastic constants increase in value with increasing pressure, reflecting that the denser structures are more resistant to strain. The eigenvalues of the stiffness tensor are positive up to 20 GPa, indicating mechanical stability of the β phase under strain. The structure at 35 GPa is the only unstable one. We conclude that the critical pressure p_c must thus be much higher than the thermodynamical transition pressure of 2.6 GPa obtained in Sec. IV B. As such, p_c can be seen as the upper bound of the phase transition pressure.

In order to estimate p_c, we further analyze our results using the Born stability criterion. As an alternative to calculating the eigenvalues of the stiffness tensor, we aim at finding a closed mathematical expression for its conditions. [29,38,39]. This can be done, for example, by making use of the leading principal minors of the stiffness tensor [29]. The onset pressure of mechanical instabilities can be estimated by evaluating these expressions over a certain pressure range. For cubic systems under hydrostatic stress, the second-order constants $B_{\gamma\delta}$ differ from the stiffness constants $C_{\gamma\delta}$ by only a linear term in P [29,38,39]. Such linear equations are not attainable for a monoclinic system. As an alternative approach, we evaluate the equation

$$\det|\boldsymbol{B}| = 0 \tag{8}$$

to explore when the system becomes unstable [39]. This enables us to estimate the critical pressures only from the stiffness tensor under load. In the case of β-Ga_2O_3, Eq. (8) is a polynomial equation of sixth degree in pressure, which can be expressed in the following form:

$$\underbrace{\left[P^2 - P\,(C_{44}+C_{66}) + C_{44}\,C_{66} - C_{46}^2\right]}_{M(P)} \cdot \underbrace{\mathcal{P}_4(P)}_{N(P)} = 0. \tag{9}$$

The first term, denoted as $M(P)$, includes only shear components of the stiffness tensor and can be identified as a shear instability criterion. The second term, $\mathcal{P}_4(P)$, is a polynomial

TABLE III. Calculated second-order elastic constants at ambient pressure for the α phase of Ga_2O_3 (in GPa) compared to previously published theoretical results.

α-Ga_2O_3	C_{11}	C_{12}	C_{13}	C_{14}	C_{33}	C_{44}
Present work	380.3	174.5	128.5	−16.6	342.9	80.1
Theory [20]	381.5	173.6	126.0	−17.3	345.8	79.7

TABLE IV. Calculated elastic moduli (in GPa) given as Voigt's, Reuss's, and Hill's averages. For the bulk modulus we also show the value obtained from the Birch-Murnaghan (B-M) EOS in Fig. 2.

β-Ga_2O_3	B	G	E	ν
Voigt	169.4	78.4	203.7	0.30
Reuss	166.7	66.2	175.3	0.32
Hill	168.0	72.3	189.6	0.31
B-M EOS	168.8			
α-Ga_2O_3	B	G	E	ν
Voigt	218.5	97.4	254.5	0.31
Reuss	216.4	92.2	242.0	0.31
Hill	217.4	94.8	248.2	0.31
B-M EOS	218.4			

of order 4 in P [denoted as $N(P)$] which is provided in the Appendix. The structure is mechanically unstable if one term equals zero. We now estimate the critical pressure(s) by interpolating our results for $M(P)$ and $N(P)$. By doing so, we can identify from the zero of $M(P)$ whether the transition occurs solely due to shear strain. Our interpolation of both expressions should be used with caution for very high (>50 GPa) and very low pressures (<−20 GPa). We want to emphasize that the aim is to estimate the critical pressure in the experimentally relevant range of up to 50 GPa. The results are illustrated in Fig. 3. We obtain two critical pressures of $p_c = -21.4$ GPa and $p_c = 32.4$ GPa. This indicates that β-Ga_2O_3 is mechanically stable in the range of $-21.4 < P < 32.4$ GPa. The upper bound agrees well with the observations from several experiments as the phase transition is fully completed above 30 to 40 GPa; that is, only α-Ga_2O_3 remains in the sample [13–15]. Only in Ref. [21] was a theoretical critical pressure below 30 GPa reported. Their transition pressure of 19.4 GPa is, however, drastically higher than our calculated value of 2.6 GPa. Note that our results are obtained at 0 K. First-principles calculations show that the elastic constants for β-Ga_2O_3 decrease with temperature; however, the effect is small at room temperature [40]. Therefore, we do not expect a significant change in the critical pressure at ambient temperature. The lower bound would indicate the emergence of another metastable phase below −21.4 GPa which is due to an instability of the pure shear criterion, $M(P) = 0$. To our knowledge, no studies have been performed with negative pressure for any of the sesquioxides. In principle, it is possible to reach negative pressure values on the order of a couple of gigapascals in solids [41].

While most studies report the phase transition with quasi-hydrostatic pressure mediums, the phase transition also occurs under nonhydrostatic conditions [14]. This, in turn, indicates that an additional mechanical instability may arise from nonuniform stress, which would reduce the symmetry of the stiffness tensor under load $\boldsymbol{B}$. We have so far not considered this in our analysis.

V. SUMMARY

We have investigated the structural and elastic properties of Ga_2O_3 in the rhombohedral α and monoclinic β phases from first principles. Based on our results, a phase transition from

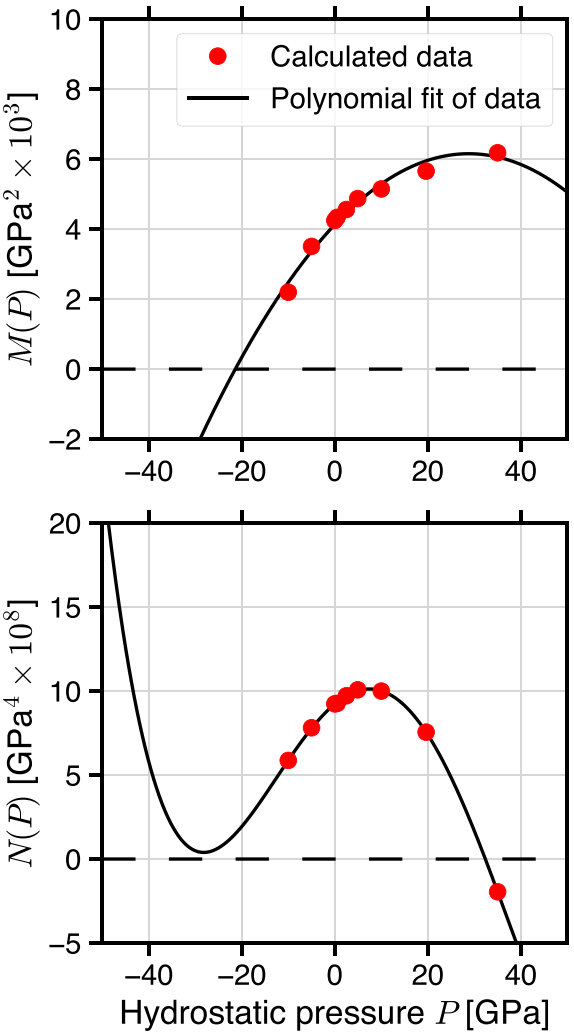

FIG. 3. Instability criteria $M(P)$ and $N(P)$, as defined in Eq. (9), as a function of hydrostatic pressure P. The red dots represent the calculated data points for the strained β-Ga_2O_3 structures. The solid lines indicate polynomial fits of order 2 and 4 to the data points for $M(P)$ and $N(P)$, respectively.

β- to α-Ga_2O_3 is energetically favored at $p_t = 2.6$ GPa. The calculated full stiffness tensors $\boldsymbol{C}$ of both phases at ambient pressure show pronounced anisotropy as well as susceptibility to shear strain, indicated by the small shear moduli of $G_V^\beta = 78$ GPa and $G_V^\alpha = 97$ GPa, respectively. Investigating the variation of the stiffness tensor under hydrostatic pressure, we observe that, according to the Born stability criterion, β-Ga_2O_3 becomes mechanically unstable at a critical pressure of $p_c = 32.4$ GPa. The transition pressure p_t can be seen as a lower bound for the phase transition and agrees well with the transition onset in previously reported experimental and theoretical results [14,16,18,20]. Considering only this pressure value obtained from thermodynamics is, however, not sufficient to explain the full range of experimentally observed transition pressures. While a phase transition is energetically favored above p_t, there are additional kinetic barriers that must be overcome. Only when the β phase is mechanically unstable, i.e., at $p_c = 32.4$ GPa, can we expect the phase transition to be completed. This agrees well with experimental

TABLE V. Second-order elastic constants of β-Ga_2O_3 as a function of hydrostatic pressure P. Pressure and elastic constants are given in gigapascals. V_0 is the volume of the unstressed crystal.

P	V/V_0	B_{11}	B_{12}	B_{13}	B_{15}	B_{22}	B_{23}	B_{25}	B_{33}	B_{35}	B_{44}	B_{46}	B_{55}	B_{66}
−10.0	1.07	175.9	90.6	84.9	−15.0	272.3	37.8	13.8	277.3	5.3	25.8	7.6	66.7	87.4
−5.0	1.03	201.5	103.7	106.0	−15.2	302.4	58.2	12.9	303.0	6.6	40.9	13.2	66.7	90.0
0.0	1.00	220.5	116.4	128.3	−17.3	329.5	79.1	11.4	326.8	7.2	50.0	18.1	66.1	91.5
0.5	0.99	222.2	117.2	131.7	−18.4	332.2	79.6	10.3	328.8	7.2	50.9	18.2	65.8	91.7
2.5	0.99	229.3	122.6	140.0	−18.8	343.4	87.7	10.8	336.3	7.7	53.6	19.4	65.4	92.1
4.9	0.97	236.3	129.9	149.7	−19.0	357.1	98.5	11.5	343.9	8.8	57.1	20.2	64.9	92.5
10.0	0.95	249.8	143.7	174.5	−23.9	382.5	118.4	8.6	361.7	9.2	61.0	22.5	62.4	92.7
19.6	0.91	265.2	170.2	222.3	−33.7	429.7	160.3	4.1	392.2	10.4	68.3	24.2	56.5	91.4
35.0	0.86	279.5	212.5	307.0	−52.9	502.4	229.5	−3.0	433.7	11.5	78.9	22.2	43.7	84.6

observations showing completion of the transition only above 30 GPa [14–16]. In addition, we found a critical pressure of −21.4 GPa. Phonon calculations in this pressure range could provide insight into the emergence of a novel metastable phase for negative pressures. Experiments with negative pressures, at values below a few gigapascals, have so far not been conducted but could point to novel discoveries in the future.

Our first-principles approach, successfully demonstrated here for the wide-gap oxide Ga_2O_3, although requiring hydrostatic pressure, is independent of crystal symmetry and thus could be applied to other materials. For example, a similar analysis could be conducted for other sesquioxides to estimate stability windows and the possible emergence of novel metastable phases.

All input and output files are available at the NOMAD Repository [42,43] with the following Ref. [44].

ACKNOWLEDGMENTS

This work was performed in the framework of GraFOx, a Leibniz-Science Campus partially funded by the Leibniz Association. The authors acknowledge the North-German Supercomputing Alliance (HLRN) for providing high-performance computing resources that contributed to the research results reported in this paper. The authors would like to thank M. Troppenz for critically reading the manuscript.

APPENDIX

The term $N(P)$ in Eq. (9) is a polynomial of order 4 in P and can be expressed in terms of the elastic constants $C_{\gamma\lambda}$ as follows:

$$N(P) = b_4 P^4 + b_3 P^3 + b_2 P^2 + b_1 P + b_0,$$

with

$$\begin{aligned}
b_4 &= -4,\\
b_3 &= -4C_{12} - 4C_{13} - 4C_{23} + 4C_{55},\\
b_2 &= C_{11}C_{22} + 2C_{11}C_{23} + C_{11}C_{33} - C_{12}^2 - 2C_{12}C_{13} - 2C_{12}C_{23} + 2C_{12}C_{33} + 4C_{12}C_{55} - C_{13}^2 + 2C_{13}C_{22}\\
&\quad - 2C_{13}C_{23} + 4C_{13}C_{55} - 4C_{15}C_{25} - 4C_{15}C_{35} + C_{22}C_{33} - C_{23}^2 + 4C_{23}C_{55} - 4C_{25}C_{35},\\
b_1 &= -C_{11}C_{22}C_{33} - C_{11}C_{22}C_{55} + C_{11}C_{23}^2 - 2C_{11}C_{23}C_{55} + C_{11}C_{25}^2 + 2C_{11}C_{25}C_{35} - C_{11}C_{33}C_{55}\\
&\quad + C_{11}C_{35}^2 + C_{12}^2C_{33} + C_{12}^2C_{55} - 2C_{12}C_{13}C_{23} + 2C_{12}C_{13}C_{55} - 2C_{12}C_{15}C_{25} - 2C_{12}C_{15}C_{35}\\
&\quad + 2C_{12}C_{23}C_{55} - 2C_{12}C_{25}C_{35} - 2C_{12}C_{33}C_{55} + 2C_{12}C_{35}^2 + C_{13}^2C_{22} + C_{13}^2C_{55} - 2C_{13}C_{15}C_{25}\\
&\quad - 2C_{13}C_{15}C_{35} - 2C_{13}C_{22}C_{55} + 2C_{13}C_{23}C_{55} + 2C_{13}C_{25}^2 - 2C_{13}C_{25}C_{35} + C_{15}^2C_{22} + 2C_{15}^2C_{23}\\
&\quad + C_{15}^2C_{33} + 2C_{15}C_{22}C_{35} - 2C_{15}C_{23}C_{25} - 2C_{15}C_{23}C_{35} + 2C_{15}C_{25}C_{33} - C_{22}C_{33}C_{55}\\
&\quad + C_{22}C_{35}^2 + C_{23}^2C_{55} - 2C_{23}C_{25}C_{35} + C_{25}^2C_{33},\\
b_0 &= C_{11}C_{22}C_{33}C_{55} - C_{11}C_{22}C_{35}^2 - C_{11}C_{23}^2C_{55} + 2C_{11}C_{23}C_{25}C_{35} - C_{11}C_{25}^2C_{33} - C_{12}^2C_{33}C_{55}\\
&\quad + C_{12}^2C_{35}^2 + 2C_{12}C_{13}C_{23}C_{55} - 2C_{12}C_{13}C_{25}C_{35} - 2C_{12}C_{15}C_{23}C_{35} + 2C_{12}C_{15}C_{25}C_{33}\\
&\quad - C_{13}^2C_{22}C_{55} + C_{13}^2C_{25}^2 + 2C_{13}C_{15}C_{22}C_{35} - 2C_{13}C_{15}C_{23}C_{25} - C_{15}^2C_{22}C_{33} + C_{15}^2C_{23}^2.
\end{aligned}$$

[1] Y. Huang, S. Yue, Z. Wang, Q. Wang, C. Shi, Z. Xu, X. D. Bai, C. Tang, and C. Gu, Preparation and electrical properties of ultrafine Ga_2O_3 nanowires, J. Phys. Chem. B **110**, 796 (2006).

[2] S. P. Arnold, S. M. Prokes, F. K. Perkins, and M. E. Zaghloul, Design and performance of a simple, room-temperature Ga_2O_3 nanowire gas sensor, Appl. Phys. Lett. **95**, 103102 (2009).

[3] N. D. Cuong, Y. W. Park, and S. G. Yoon, Microstructural and electrical properties of Ga_2O_3 nanowires grown at various temperatures by vapour-liquid-solid technique, Sens. Actuators, B **140**, 240 (2009).

[4] Z. Liu, T. Yamazaki, Y. Shen, T. Kikuta, N. Nakatani, and Y. Li, O_2 and CO sensing of Ga_2O_3 multiple nanowire gas sensors, Sens. Actuators, B **129**, 666 (2008).

[5] L. Mazeina, F. K. Perkins, V. M. Bermudez, S. P. Arnold, and S. M. Prokes, Functionalized Ga_2O_3 nanowires as active material in room temperature capacitance-based gas sensors, Langmuir **26**, 13722 (2010).

[6] P.-C. Chang, Z. Fan, W.-Y. Tseng, A. Rajagopal, and J. G. Lu, β-Ga_2O_3 nanowires: Synthesis, characterization, and p-channel field-effect transistor, Appl. Phys. Lett. **87**, 222102 (2005).

[7] P. Feng, J. Y. Zhang, Q. H. Li, and T. H. Wang, Individual β-Ga_2O_3 nanowires as solar-blind photodetectors, Appl. Phys. Lett. **88**, 153107 (2006).

[8] L. Li, E. Auer, M. Liao, X. Fang, T. Zhai, U. K. Gautam, A. Lugstein, Y. Koide, Y. Bando, and D. Golberg, Deep-ultraviolet solar-blind photoconductivity of individual gallium oxide nanobelts, Nanoscale **3**, 1120 (2011).

[9] Y. Kokubun, K. Miura, F. Endo, and S. Nakagomi, Sol-gel prepared β-Ga_2O_3 thin films for ultraviolet photodetectors, Appl. Phys. Lett. **90**, 031912 (2007).

[10] W. Y. Weng, T. J. Hsueh, S. J. Chang, G. J. Huang, and S. P. Chang, A solar-blind β-Ga_2O_3 nanowire photodetector, IEEE Photonics Technol. Lett. **22**, 709 (2010).

[11] R. Roy, V. G. Hill, and E. F. Osborn, Polymorphism of Ga_2O_3 and the system $Ga_2O_3-H_2O$, J. Am. Chem. Soc. **74**, 719 (1952).

[12] J. P. Remeika and M. Marezio, Growth of α-Ga_2O_3 single crystals at 44 kbars, Appl. Phys. Lett. **8**, 87 (1966).

[13] K. E. Lipinska-Kalita, B. Chen, M. B. Kruger, Y. Ohki, J. Murowchick, and E. P. Gogol, High-pressure x-ray diffraction studies of the nanostructured transparent vitroceramic medium $K_2O-SiO_2-Ga_2O_3$, Phys. Rev. B **68**, 035209 (2003).

[14] K. E. Lipinska-Kalita, P. E. Kalita, O. A. Hemmers, and T. Hartmann, Equation of state of gallium oxide to 70 GPa: Comparison of quasihydrostatic and nonhydrostatic compression, Phys. Rev. B **77**, 094123 (2008).

[15] H. Wang, Y. He, W. Chen, Y. W. Zeng, K. Stahl, T. Kikegawa, and J. Z. Jiang, High-pressure behavior of β-Ga_2O_3 nanocrystals, J. Appl. Phys. **107**, 033520 (2010).

[16] D. Machon, P. F. McMillan, B. Xu, and J. Dong, High-pressure study of the β-to-α transition in Ga_2O_3, Phys. Rev. B **73**, 094125 (2006).

[17] H. Kishimura and H. Matsumoto, Evaluation of the shock-induced phase transition in β-Ga_2O_3, Jpn. J. Appl. Phys. **57**, 125503 (2018).

[18] P. Kroll, Spinel-type gallium oxynitrides attainable at high pressure and high temperature, Phys. Rev. B **72**, 144407 (2005).

[19] F. Litimein, D. Rached, R. Khenata, and H. Baltache, FPLAPW study of the structural, electronic, and optical properties of Ga_2O_3: Monoclinic and hexagonal phases, J. Alloys Compd. **488**, 148 (2009).

[20] J. Furthmüller and F. Bechstedt, Quasiparticle bands and spectra of Ga_2O_3 polymorphs, Phys. Rev. B **93**, 115204 (2016).

[21] S. Luan, L. Dong, and R. Jia, Analysis of the structural, anisotropic elastic and electronic properties of β-Ga_2O_3 with various pressures, J. Cryst. Growth **505**, 74 (2019).

[22] S. Timoshenko, *Theory of Elasticity* (McGraw-Hill, New York, 1951).

[23] D. C. Wallace, *Thermodynamics of Crystals* (Wiley, New York, 1972).

[24] L. D. Landau and E. M. Lifschitz, *Theory of Elasticity* (Elsevier, Amsterdam, 1986).

[25] R. Golesorkhtabar, P. Pavone, J. Spitaler, P. Puschnig, and C. Draxl, Elastic: A tool for calculating second-order elastic constants from first principles, Comput. Phys. Commun. **184**, 1861 (2013).

[26] G. Grimvall, B. Magyari-Köpe, V. Ozoliņš, and K. A. Persson, Lattice instabilities in metallic elements, Rev. Mod. Phys. **84**, 945 (2012).

[27] D. C. Wallace, Thermoelasticity of stressed materials and comparison of various elastic constants, Phys. Rev. **162**, 776 (1967).

[28] M. Born, On the stability of crystal lattices. I, Math. Proc. Cambridge Philos. Soc. **36**, 160 (1940).

[29] F. Mouhat and F.-X. Coudert, Necessary and sufficient elastic stability conditions in various crystal systems, Phys. Rev. B **90**, 224104 (2014).

[30] A. Gulans, S. Kontur, C. Meisenbichler, D. Nabok, P. Pavone, S. Rigamonti, S. Sagmeister, U. Werner, and C. Draxl, `exciting`: A full-potential all-electron package implementing density-functional theory and many-body perturbation theory, J. Phys.: Condens. Matter **26**, 363202 (2014).

[31] J. P. Perdew, A. Ruzsinszky, G. I. Csonka, O. A. Vydrov, G. E. Scuseria, L. A. Constantin, X. Zhou, and K. Burke, Restoring the Density-Gradient Expansion for Exchange in Solids and Surfaces, Phys. Rev. Lett. **100**, 136406 (2008).

[32] M. Råsander and M. A. Moram, On the accuracy of commonly used density functional approximations in determining the elastic constants of insulators and semiconductors, J. Chem. Phys. **143**, 144104 (2015).

[33] H. He, R. Orlando, M. A. Blanco, R. Pandey, E. Amzallag, I. Baraille, and M. Rérat, First-principles study of the structural, electronic, and optical properties of Ga_2O_3 in its monoclinic and hexagonal phases, Phys. Rev. B **74**, 195123 (2006).

[34] F. Giustino, *Materials Modelling Using Density Functional Theory: Properties and Predictions* (Oxford University Press, Oxford, 2014).

[35] K. Karch, F. Bechstedt, P. Pavone, and D. Strauch, Pressure-dependent properties of SiC polytypes, Phys. Rev. B **53**, 13400 (1996).

[36] M. Yan-Mei, C. Hai-Yong, Y. Kai-Feng, L. Min, C. Qi-Liang, L. Jing, and Z. Guang-Tian, High-pressure and high-temperature behaviour of gallium oxide, Chin. Phys. Lett. **25**, 1603 (2008).

[37] K. Adachi, H. Ogi, N. Takeuchi, N. Nakamura, H. Watanabe, T. Ito, and Y. Ozaki, Unusual elasticity of monoclinic β-Ga_2O_3, J. Appl. Phys. **124**, 085102 (2018).

[38] J. Wang, S. Yip, S. R. Phillpot, and D. Wolf, Crystal Instabilities at Finite Strain, Phys. Rev. Lett. **71**, 4182 (1993).

[39] J. Wang, J. Li, S. Yip, S. Phillpot, and D. Wolf, Mechanical instabilities of homogeneous crystals, Phys. Rev. B **52**, 12627 (1995).

[40] M. Santia, N. Tandon, and J. Albrecht, Effects of strain on the optical and thermodynamic properties of β-Ga_2O_3, Solid State Commun. **297**, 1 (2019).

[41] A. R. Imre, On the existence of negative pressure states, Phys. Status Solidi B **244**, 893 (2007).

[42] C. Draxl and M. Scheffler, NOMAD: The FAIR concept for big data-driven materials science, MRS Bulletin **43**, 676 (2018).

[43] C. Draxl and M. Scheffler, The NOMAD laboratory: From data sharing to artificial intelligence, J. Phys. Mater. **2**, 036001 (2019).

[44] https://dx.doi.org/10.17172/NOMAD/2021.12.02-1.